

# An investigation of high-order harmonics in the pressure field around a vertical cylinder in steep wave conditions

Haoyu Ding<sup>a</sup>, Jun Zang<sup>a</sup>, Tianning Tang<sup>b</sup>, Paul H. Taylor<sup>c</sup>, Thomas A.A. Adcock<sup>b</sup>, Guangwei Zhao<sup>d</sup>, Saishuai Dai<sup>d</sup>

a. Department of Architecture and Civil Engineering, University of Bath, UK

b. Department of Engineering Science, University of Oxford, Oxford, UK

c. Oceans Graduate School, The University of Western Australia, Crawley, Australia

d. Naval Architecture, Ocean and Marine Engineering Department, University of Strathclyde, Glasgow, UK

Email: hd484@bath.ac.uk

## 1 Introduction

Offshore structures, encompassing foundations for offshore wind turbines, supports for marine renewable energy devices, bridge piers, and floating vessels, are consistently subjected to severe environmental loads. These loads often dictate the design criteria. Understanding the physics and statistics of wave-structure interaction, especially under non-linear loads experienced in extreme conditions, remains a complex and partially unresolved challenge. Notably, secondary load cycles significantly contribute to the 'ringing' responses in cylindrical structures, as discussed in previous studies (e.g., Grue et al. (1993), Chaplin et al. (1997)). This paper focuses on analysing loads in focused wave groups, representing short-term extreme wave conditions, on bottom-mounted vertical cylinders relevant to fixed offshore wind turbines. Pressure contour plots over the cylinder's surface were previously examined by Ghadirian & Bredmose (2020) while studying secondary load cycles. In this research, we adopt the phase-based harmonic separation method for wave forces (Fitzgerald et al. (2014)) to analyse the pressure contour plots. This method effectively isolates harmonic pressure components from the total pressures, enabling a novel exploration of the mechanisms behind secondary load cycles from the perspective of high-order harmonics on the cylinder surface.

## 2 Numerical Method

In this study, computational fluid dynamics (CFD) results are analysed. OpenFOAM, a well-known open-source model, has been used for this task. The waves2foam toolbox, as described in Jacobsen et al. (2012), is used for wave generation, offering accurate simulation of the wave conditions for our study. A Reynolds-averaged Navier–Stokes (RANS) model is employed for wave-structure interaction simulations. Chen et al. (2014) conducted a series of mesh convergence tests to determine the optimal mesh size for accurate prediction of wave-cylinder interactions. This study employs the same mesh configuration, but with further refinement to the innermost layer around the cylinder to 0.2 times the mesh size used by Chen et al. (2014). This refinement enhances the capture of spatially and temporally localised wave behaviours, such as the steep gradient of wave run-up on the cylinder and secondary load cycles.

A physical experiment conducted at the Danish Hydraulic Institute (DHI) (Chen et al. (2018)) serves to validate the numerical model. In this experiment, a fixed cylinder with a

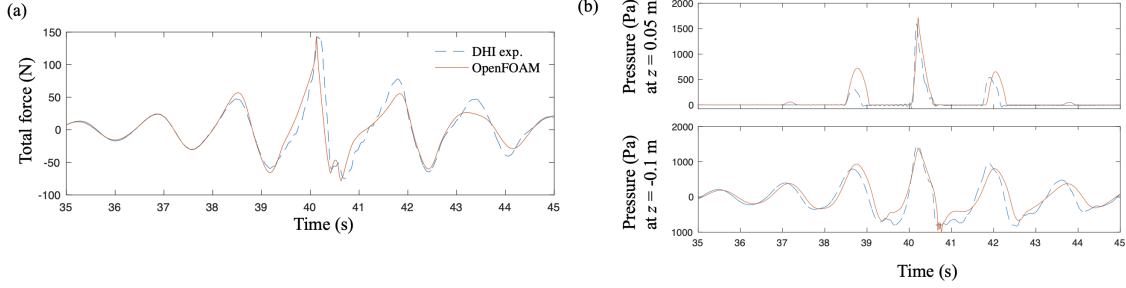


Figure 1: (a) Validation of OpenFOAM predictions showing total inline force exerted on the cylinder. (b) Validation through point pressure measurements.

radius of 0.125 m was subjected to extreme focused waves in a wave tank with a depth of 0.505 m. The wave parameters were a main crest amplitude of 0.15 m, a peak wave period of 1.64 s, and a wave number of 1.98/m. Figure 1(a) and (b) present comparative results for total force and point pressures, respectively. For total force, the OpenFOAM results show good agreement with the experimental data. Under the impact of extreme waves, wave slamming loads are noticeable in the main peak, and distinct secondary load cycles appear in the first trough following the main peak. These phenomena observed in the physical experiments are also accurately predicted by OpenFOAM. In contrast to the total force, which is an integrated result, point pressure measurements are more sensitive and challenging to predict. Nonetheless, OpenFOAM successfully predicts similar pressure distributions at various stagnation points up the front of the cylinder, denoted by  $Z$ , where  $Z = 0$  corresponds to the still water level,  $Z < 0$  represents submersion. These comparisons provide strong evidence that OpenFOAM is capable of accurately simulating wave loading and pressure under severe wave conditions, thereby allowing subsequent investigations into secondary load cycles.

### 3 Results

A series of new experiments were carried out at the Kelvin Hydrodynamics Laboratory, University of Strathclyde, using a bottom-mounted, surface-piercing vertical cylinder with a radius ( $R$ ) of 0.2 m in a constant water depth of 1.8 m. This research provides CFD simulations for these tests. Comparisons to the experiments will be reported at the workshop. Specifically, a focused wave group based on the JONSWAP spectrum ( $\gamma = 3.3$ ) was selected for detailed analysis. This wave group is characterized by a main crest amplitude ( $A$ ) of 0.41 m, a peak wave period ( $T$ ) of 2.5 s, and a peak wave number ( $k$ ) of 0.74/m, serving as a representative example for this section.

#### 3.1 Scattering Pressure

The scattering pressure is calculated by subtracting the baseline pressure (measured in the wave but without the cylinder) from the total pressure recorded when the cylinder is present. To facilitate this, the pressures at mesh points on the surface of a cylinder are outputted in the OpenFOAM simulation. Pressures are also taken from these same locations in a simulation with the cylinder removed and replaced by water to gauge the scattering pressure contributions from incident waves and hydrostatic pressure alone.

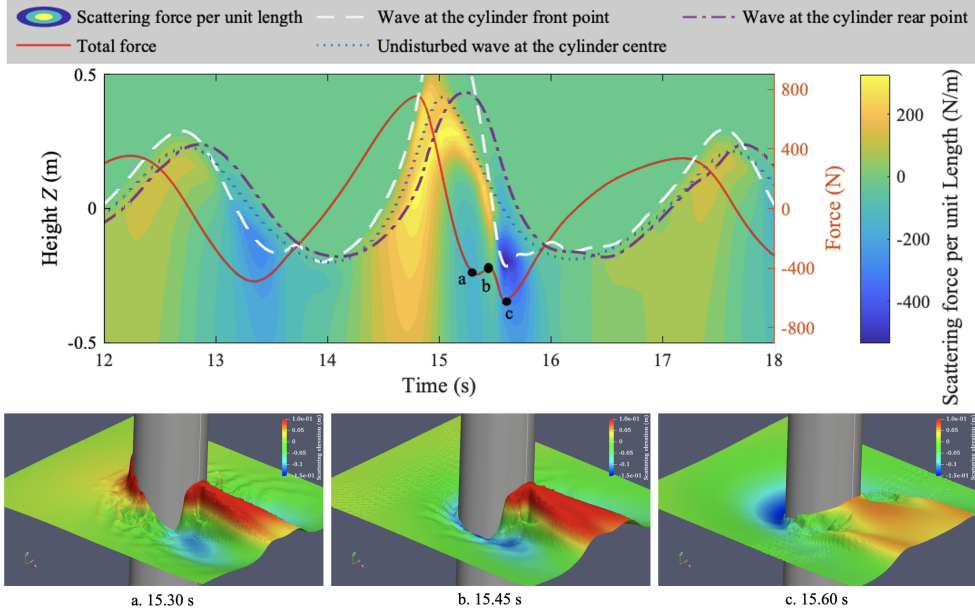


Figure 2: Contour plot of inline scattering force per unit length against cylinder height and time, with overlaying time histories of total force (red line). Also depicted are the total free surface elevations along the cylinder’s central line, from the front (white dashed line) to the rear (purple dash-dot line), and undisturbed wave elevations at the centre point in the absence of the cylinder (blue dotted line). The scattering wave field around the cylinder is shown at three time points: (a) 15.30 s, (b) 15.45 s, and (c) 15.60 s.

The scattering wave field, depicted in Figure 2, represents the difference between the total waves and the undisturbed waves, and is derived using the same methodology.

The inline scattering force per unit length vertically is found from the circumferential integral of the local scattering pressure resolved along the inline direction. This is visualised in a contour plot against time and the vertical elevation in Figure 2. Accompanying the contour is the total force. A secondary load cycle is apparent in the total force trace around 15.5 seconds. Regarding the scattering force per unit length contour plot, a negative ‘chamber’ emerges below the positive region at  $Z = 0.2m$  around 15 s, marking the onset of the secondary load cycle. A positive region, termed a ‘positive insertion’, transiently inserts into the negative zone as a minor crest appears in the trough of the total force, followed by a substantial negative region around  $Z = -0.2m$ . Three critical points during the force trough are labeled as a, b, and c in Figure 2. The scattering fields at these points, along with the central line free surface elevations, illustrate the free surface behaviours during the secondary load cycle. The significant wave run-up at point a and the wave set-down at point c at the cylinder’s front stagnation point are observed, which may contribute to the variations in force. These variations in the scattering force per unit length highlight the pressure field’s sensitivity around the cylinder to secondary load cycles, suggesting that abrupt shifts from positive to negative pressures could have significant implications for structural fatigue.

### 3.2 Pressure Decomposition

The four-phase harmonic separation method proposed by Fitzgerald et al. (2014) has been demonstrated as effective in decomposing individual force harmonics when the hy-

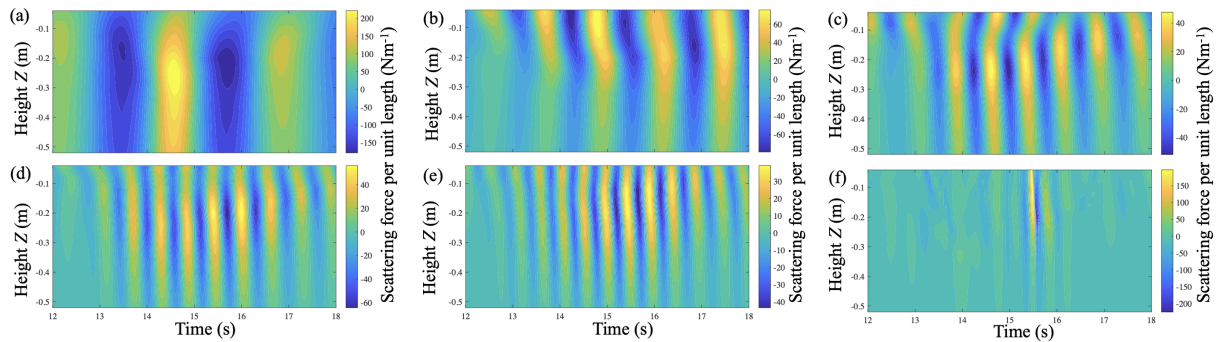


Figure 3: Contour plots of inline scattering force per unit length for (a) linear harmonic, (b) second harmonic, (c) third harmonic, (d) fourth harmonic, (e) fifth harmonic and (f) beyond fifth harmonic

hydrodynamic force in focused waves possesses a Stokes-like structure. In this research, this method is also applied to the point pressures on the cylinder surface, facilitating the integration of contour plots for inline scattering force per unit length across individual harmonics. Evidence supporting the method's applicability to pressure measurements will be presented at the workshop. Figure 3 displays the results following this decomposition on the force per unit length below the still water level. The oscillation between positive and negative regions in these contour plots accurately reflects the relationship between harmonics from first to fifth order, with their magnitudes generally diminishing with higher harmonic. Notably, harmonics beyond the fifth harmonic still show significant magnitudes with negative regions ( $-224 \text{ N/m}$ ) exceeding the linear scattering force per unit length ( $-178 \text{ N/m}$ ). The pronounced values of these high harmonics, particularly evident around  $15.5 \text{ s}$ , correspond with the 'positive insertion' identified in Figure 2 and may also influence secondary load cycles. This decomposition underscores the critical influence of higher-order harmonics on the scattering force amid severe wave conditions and suggests that components beyond the fifth harmonic have substantial implications for secondary load cycles.

## References

- Chaplin, J. R., Rainey, R. C. T. & Yemm, R. W. (1997), 'Ringing of a vertical cylinder in waves', *J. Fluid Mech.* pp. 119–147.
- Chen, L. F., Zang, J., Hillis, A. J., Morgan, G. C. & Plummer, A. R. (2014), 'Numerical investigation of wave-structure interaction using OpenFOAM', *Ocean Eng.* **88**, 91–109.
- Chen, L., Zang, J., Taylor, P. H., Sun, L., Morgan, G., Grice, J., Orszaghova, J. & Ruiz, M. T. (2018), 'An experimental decomposition of nonlinear forces on a surface-piercing column: Stokes-type expansions of the force harmonics', *J. Fluid Mech.* **848**, 42–77.
- Fitzgerald, C. J., Taylor, P. H., Eatock Taylor, R., Grice, J. & Zang, J. (2014), 'Phase manipulation and the harmonic components of ringing forces on a surface-piercing column', *Proc. R. Soc. A* **470**(2168), 20130847.
- Ghadirian, A. & Bredmose, H. (2020), 'Detailed force modelling of the secondary load cycle', *J. Fluid Mech.* **889**, 1–30.
- Grue, J., Bjørshol, G. & Strand, Ø. (1993), 'Higher harmonic wave exciting forces on a vertical cylinder', *Preprint series. Mechanics and Applied Mathematics* <http://urn.nb.no/URN:NBN:no-23418>.
- Jacobsen, N. G., Fuhrman, D. R. & Fredsøe, J. (2012), 'A wave generation toolbox for the open-source CFD library: OpenFoam®', *Int. J. Numer. Methods Fluids* **70**, 1073–1088.